Proceedings of the World Congress on Engineering 2017 Vol II
WCE 2017, July 5-7, 2017, London, U.K.

Residual Stress Simulations of Girth Welding in Subsea Pipelines

Bridget E. Kogo, Bin Wang, Luiz C. Wrobel and Mahmoud Chizari, *Member, IAENG*

Abstract—**Numerical modelling of the welding of dissimilar materials, stainless steel and mild steel, has been carried out using Abaqus together with Gas Metal Arc Weld (GMAW) in order to provide a better understanding of the transient temperature profiles and the stress distribution in a pipe. The results clearly show that the temperature distribution in the modelled pipe is a function of the thermal conductivity of each weld metal as well as the distance away from the heat source. Results also clearly show agreement with previous findings.**

Index Terms—Transient temperature response, dissimilar material joint, FEA, girth weld

I. Introduction

WELDING of cylindrical objects is complex and poses a source of concern in manufacturing processes. There are several benefits of welding as a joining technology which includes cost effectiveness, flexibility in design, enhanced structural integrity, and composite weight reduction. However, thermal stresses are usually initiated on the weld and the base metal [1-4]. Poorly welded joints result in leakages, pipe failures and bursts, which lead to possible environmental hazards, loss of lives and properties. Welding of dissimilar materials is carried out in-house by using GMAW, and an FEA analysis was carried out on pipe models having different clad thicknesses of 2mm and 12mm, respectively, and the temperature versus distance profile obtained. The 12mm cladded pipe results are discussed in this paper.

The process of carrying out welding using an arc weld entails melting down the base metal and, in this research; it also involves melting down the clad metal. In the course of carrying out the welding, filler metals are also melted such that the solution formed by heating up all these materials and holding them at that range of temperature long enough permits the diffusion of constituents into the molten solution; this is followed by cooling down rapidly in order to maintain these constituents within the solution. The result of this procedure generates a metallurgical structure positioning in-situ the material which supplies superior tensile strength. The bulk of the material immediately after the fusion zone (FZ), which has its characteristics altered by the weld, is termed Heat Affected Zone (HAZ). Referring to Figures 5 (a) and 13, the volume of material within the HAZ undergoes considerable change which could be advantageous to the weld joint, but in some circumstances might not be beneficial.

Manuscript received Feb 15, 2017; revised April 05, 2017.

Bridget E. Kogo (corresponding author) is with Mechanical, Aerospace and Civil Engineering Department, College of Engineering, Design and Physical Sciences, Brunel University London, UK (e-mail: biddyagada@yahoo.com)

Bin Wang is with Mechanical, Aerospace and Civil Engineering Department, College of Engineering, Design and Physical Sciences, Brunel University London, UK (e-mail: bin.wang@brunel.ac.uk)

Luiz C. Wrobel is with Mechanical, Aerospace and Civil Engineering Department, College of Engineering, Design and Physical Sciences, Brunel University London, UK (e-mail: luiz.wrobel@brunel.ac.uk)

Mahmoud Chizari is with the School of Mechanical Engineering, Sharif University of Technology in Tehran. He is also with Mechanical, Aerospace and Civil Engineering Department, College of Engineering, Design and Physical Sciences, Brunel University London, Uxbridge, UB8 3PH, UK (e-mail: mahmoudchizari@yahoo.com).

II. FE Analysis

A. Numerical Analysis

The underlying theory behind weld research is based on the Gaussian transformation principle, which states that 'A Gaussian flat surface has a Gaussian curvature at each and every point of the magnitude of zero'. Going by this principle, the surface of a cylinder can be said to be a Gaussian flat plane since it can be revolved from a piece of paper. Furthermore, the implication is that this can be done without stretching the plane, folding or tearing it. The parameter $r(u,v)$ is an orthogonal parameterization of a surface [5]. This is further illustrated in Figure 1.

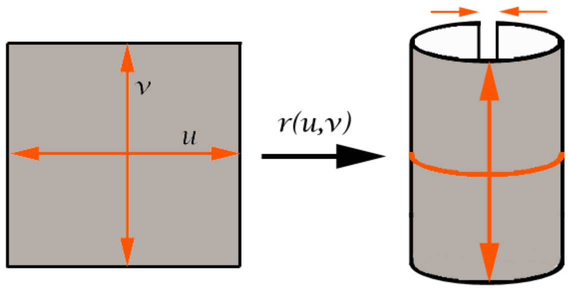

Fig. 1. Conversion of a plate of a certain dimension into a cylinder of the same dimension

This means that the thermal distributions on the surface of a cylinder can also be appreciated by studying the thermal distribution on the surface of welded plates.

For the fully cladded pipe in Figure 2, the total number of nodes in the FEA mesh is 208,640 and elements 180,306. An 8-node linear brick is generated using a hexagonal element. The section of the meshed pipe in Figure 2 which corresponds to the weld is depicted by two squares in the middle. Linear hexahedral elements are recommended for their reduced computation time and ease of running analysis due to the structured grid which makes up the mesh. All elements are identical on this structured array. Hexahedral elements guarantee minimal skewness because of their uniform grid shape; however, a hexahedral mesh can also be unstructured depending on the manner in which element indexing is executed [6].

ISBN: 978-988-14048-3-1
ISSN: 2078-0958 (Print); ISSN: 2078-0966 (Online)

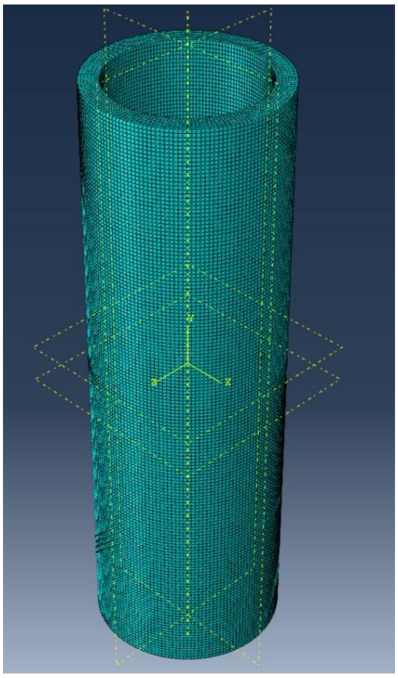

Fig. 2. Meshed pipe model using a fine type of elements. Mesh convergence was checked to make sure about the quality of the mesh size.

B. *Finite Element Models*

Figure 3 shows the thermal simulation for heat pass 1 in a full 3D pipe with different temperature contours, which are seen as thermal variations representing each thermal distribution shown in the temperature panel on the top left hand side of the figure. The first band depicts the hottest part of the weld with a temperature of 1,545^{o}C, whereas the other regions are depicted by a lower temperature leaving the bulk of the pipe at 99^{o}C. The FZ corresponds to temperatures between 1,304^{o}C to 1,545^{o}C and is depicted by the middle at the center band of the weld in Figure 3; whereas the HAZ is represented by the band to the immediate left and right of the center bands and ranges from 220^{o}C to 1,184^{o}C.

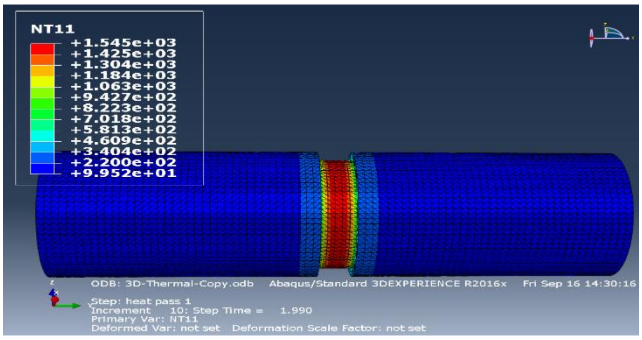

Fig. 3. 3D weld pipes showing the different weld profiles for heat pass 1. Temperature profiles of a ring weld through the weld pass length.

III. EXPERIMENTAL INVESTIGATION

A. *Tensile test*

A number of factors such as temperature, strain rate and anisotropy affect the shape of the stress- strain curves. The parent metals have different elongation characteristics, and each exhibits this at different rates because of the applied stress under which it is stretched. Similarly, the behaviour of the weld metal under the displacement time curve in Figure 4 (b) is also due to slip, which is caused by the elongation and failure of the different metals (mild steel and stainless steel) present within the weld samples, since they each have their original ultimate tensile stress (UTS). The volumetric change and yield strength in Figure 4 (a) as a result of martensitic transformation have influences on the welding residual stresses, increasing the magnitude of the residual stress in the weld zone as well as changing its sign.

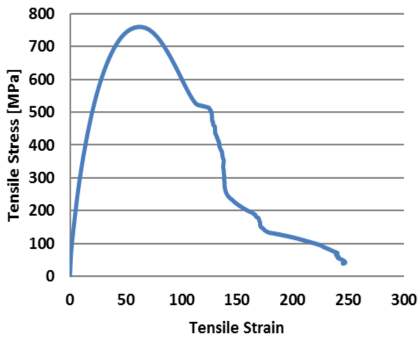

Fig. 4. (a) Stress-Strain curve of 12mm cladded pipe

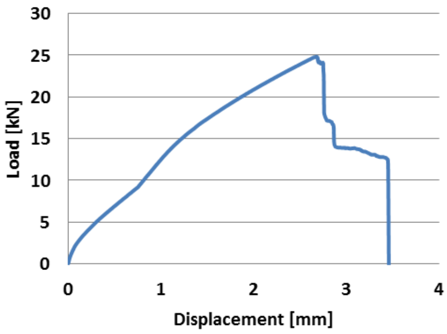

Fig. 4. (b) Force-Displacement curve of 12mm cladded pipe

B. *Microstructures*

From the result in Figure 5 (b), it is evident that there is an element of carbon in the stainless steel. The microstructure in Figure 5 (a) shows the parent metals - Stainless Steel and Mild Steel - as well as the weld in between. Table I reveals the elements present in both stainless steel and mild steel. The Fe content is higher in the mild steel than in the stainless steel. The Nickel content is very high in the stainless steel and absent in the mild steel. Likewise, the Molybdenum content is higher in the stainless steel than in the mild steel. The Cr content is very high in the stainless steel compared with the mild steel, and these can be seen in the spectrum in Figure 5 (b) for stainless steel.

TABLE I
ELEMENTS IN WELD STEEL OF 12MM SS/MS CLAD

Element	Fe	C	Cr	N	Mn	Si	Ca	Mo
SS	71.30	5.08	13.41	7.05	1.51	0.41	0.08	1.16
MS	92.02	5.51	0.61	-	1.13	0.41	0.07	0.25

ISBN: 978-988-14048-3-1
ISSN: 2078-0958 (Print); ISSN: 2078-0966 (Online)

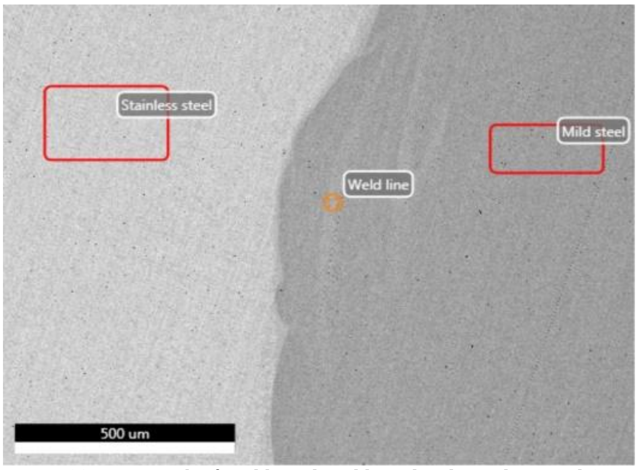

Fig. 5. (a) Micrograph of Weld Steel, Mild Steel and Stainless Steel (parent material) in 12mm SS/MS clad

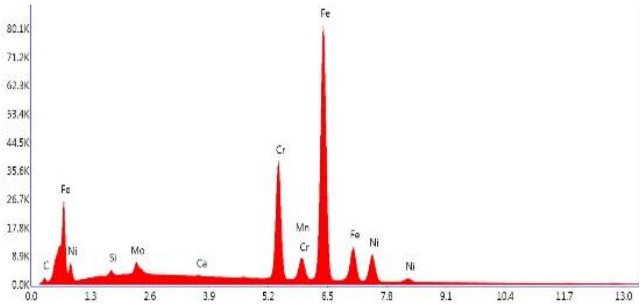

Fig. 5. (b) Spectrum of Stainless Steel (parent material) in 12mm SS/MS clad

It is known in welding that the weakest point of the weld is the clad/HAZ interface due to inconsistent fusion and reheating [7]. During butt welding, there are high thermal gradients experienced during the procedure leading to residual stress and discrepancy in hardness. The presence of residual stresses as a result of high concentration of thermal stress in the clad usually affects the inherent resistance to corrosion and fatigue cracks. In order to enhance the mechanical properties of the clad/base metal interface, as well as reduce the residual stresses generated, post-heat treatments are usually carried out.

The presence of Nickel and Manganese in steel decreases the eutectoid temperature lowering the kinetic barrier whereas Tungsten raises the kinetic barriers. The presence of Manganese increases hardness in steel and likewise Molybdenum.

Figure 5 (a) displays microstructures and elements of the 12mm weld. Within the transition zone next to the weld metal, the stainless steel part of the microstructures contains acicular ferrites, which are formed when the cooling rate is high in a melting metal surface or material boundaries. Different ferrites are formed starting from the grain boundary. Such ferrites include plate and lath Martensite, Widmanstatten ferrite, and grain boundary ferrite.

C. Weld Direction - Nomenclature

The usual concept of 90 degrees, 180 degrees, 270 degrees and 360 degrees has been used in a clockwise manner to describe the direction of the weld, as well as the 3 o'clock, 6 o'clock, 9 o'clock and 12 o'clock convention.

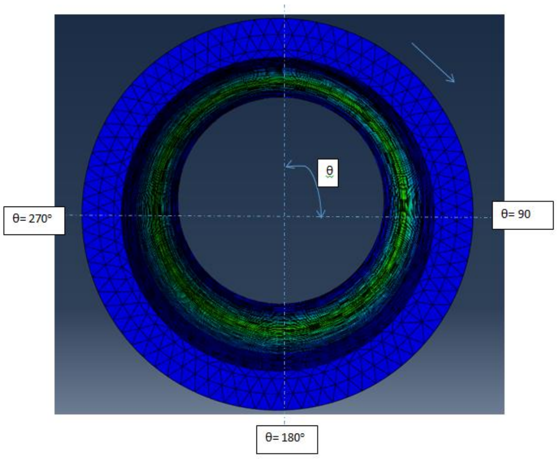

Fig.6. A representation of the pipe rotation and nomenclature of 90, 180, 270 and 360 degrees

Figure 7 illustrates the 45, 135, 225 and 315-degree reference system, which is obtained by simply rotating the cross-section of the pipe in Figure 6 through an angle of 45 degrees in the clockwise direction.

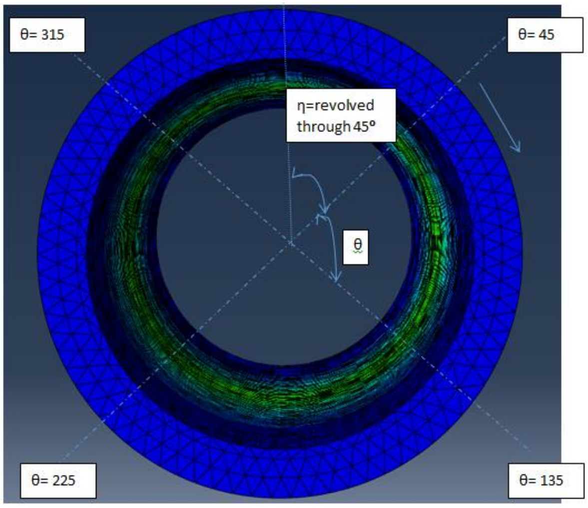

Fig. 7. A representation of the pipe rotation and nomenclature of 45, 135, 225 and 315 degrees

The above style of representation of a welding direction is known as 1:30 hours, 4:30 hours, 7:30 hours and 10:30 hours face of a clock using a temporal connotation. Representing the four positions of interest on the pipe circumference onto a plate, following the Gaussian transformation principle, the following output is obtained as shown in Figure 8. This implies that different weld directions can also be represented on a plane surface as shown on the 2D plate in Figure 8.

ISBN: 978-988-14048-3-1
ISSN: 2078-0958 (Print); ISSN: 2078-0966 (Online)

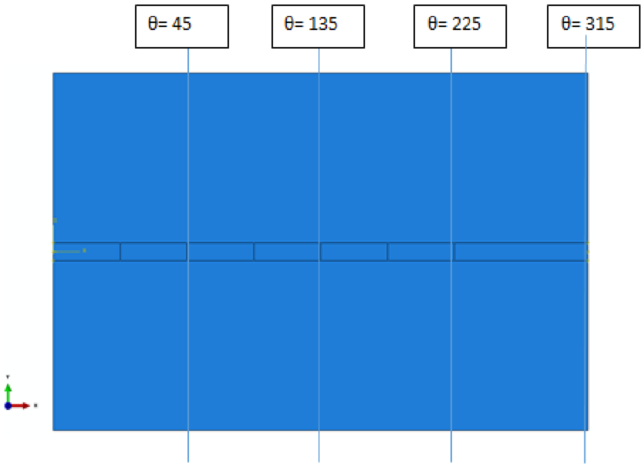

Fig. 8. A plate representation of the pipe rotation and nomenclature of 45, 135, 225 and 315 degrees convention.

IV. RESULTS AND DISCUSSION

A. Thermal Analysis

From the different plots of temperature versus distance in Figures 9-11, the effect of the clad on the weld can be seen as the clad has effectively reduced the operating temperature thereby limiting the thermal conductivity of the welded path. The reduction in thermal conductivity enhances the insulating effect of the cladding.

The thermal diffusivity varies directly with the density and specific heat of the material. This implies that, as the thickness of the insulating material increases, the thermal diffusivity reduces. The material density is directly related to the insulation performance.

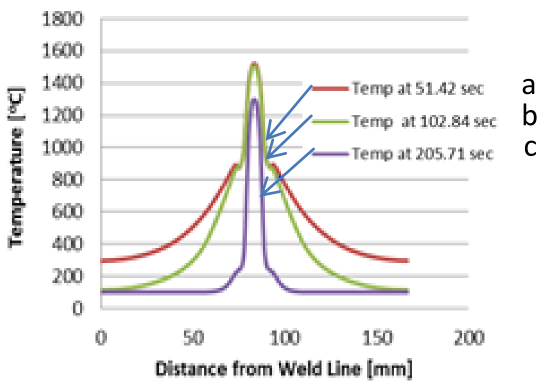

Fig. 9. Axial temperature distributions for 45° cross-section at different weld times from the weld start

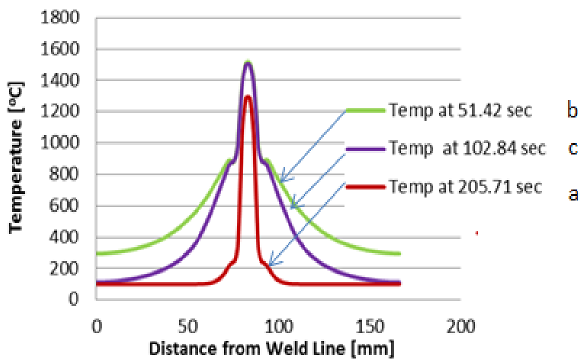

Fig. 10. Axial temperature distributions for 135° cross-section at different weld times from the weld start

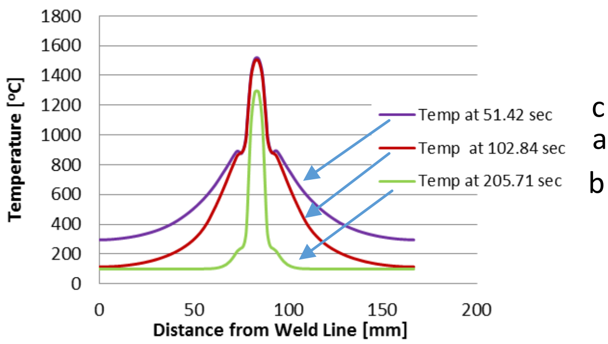

Fig. 11. Axial temperature distributions for 225° cross-section at different weld times from the weld start

Bearing in mind that the temperature imparts directly on the toughness, modulus of elasticity, ultimate tensile strength and yield stress, this means that an increased operating temperature will also impact upon these properties of the cladded pipes.

B. Stress Analysis

From Figures 12 and 14 (*a* and *b*), which display the residual axial stress in the cladded pipe, it can be seen that close to the weld vicinity, compressive and tensile stress fields are present in and near the section of the weld both on the external and internal surfaces of the pipe. Furthermore, this occurrence can be credited to the varying temperature profiles on the inner and outer surfaces of the pipe. By virtue of the thickness of the cylinder wall and being very close to the weld line (which is represented by the vertical line), tensile and compressive residual stress fields are generated due to shrinkage (Figures 15 and 17) occurring within the weld pipe. The findings in Figures 12 and 13 are similar to that in [8] and [9].

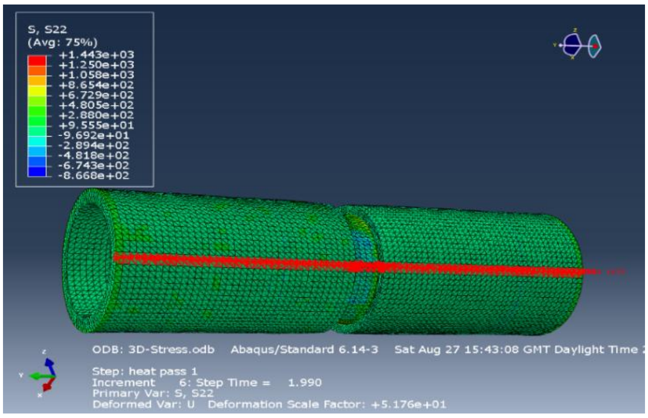

Fig. 12. A typical pipe model showing nodal values of residual stress in the S22 direction

The differences in the values of the residual stresses are a result of the different material properties such as yield strength for the base and filler metals, weld geometry and heat source parameters. There have been volumetric change and yield strength as a result of martensitic transformation, which have effects on welding residual stress, by increasing the magnitude of the residual stress in the weld zone as well as changing its sign. The simulated results show that the volumetric change and the yield strength change due to the martensitic transformation have influences on the welding residual stress.

ISBN: 978-988-14048-3-1
ISSN: 2078-0958 (Print); ISSN: 2078-0966 (Online)

Fig. 13. Welded plates showing residual tensile stress (underneath - inside pipe) and compressive stress (above – outer surface of pipe).

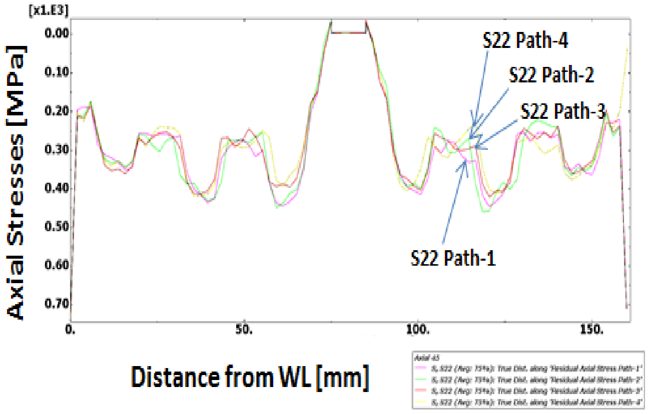

Fig. 14. (a) Residual axial stresses on the inner surface and in S22 direction of the HAZ of the 12 mm clad pipes

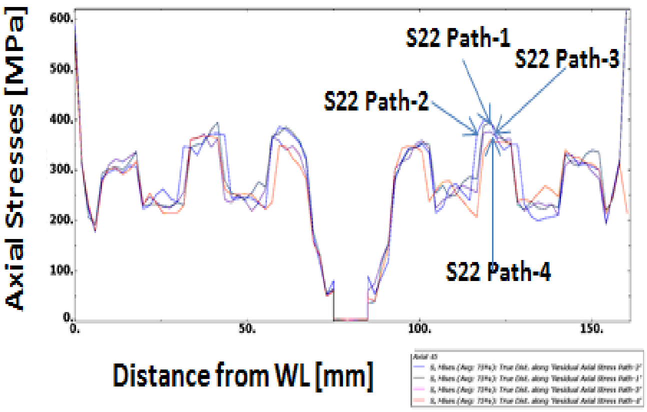

Fig. 14. (b) Residual axial stresses versus distance curve on the outer surface of the HAZ of the 12 mm clad pipes

C. Radial Shrinkage

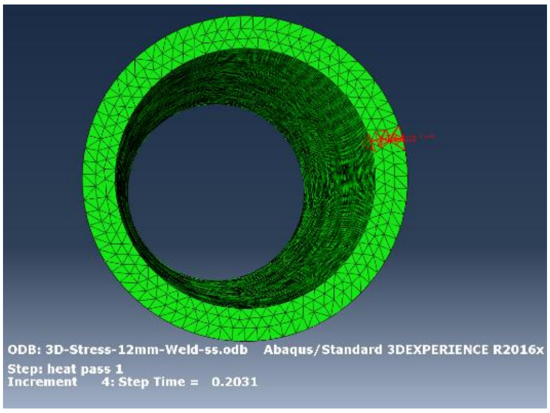

Fig. 15. A typical pipe model showing nodal readings for radial shrinkage

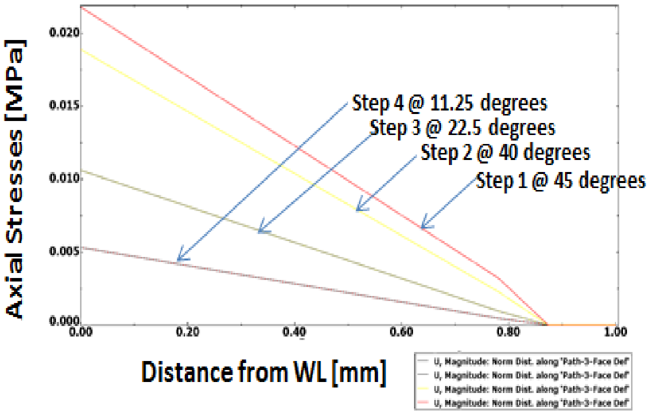

Fig. 16. Radial shrinkage versus normalized distance curve on the outer surface of the 12 mm clad pipe end

When the weldment cools down, there is usually an axial inclination of the constraint free end of the pipe taking place.The thickness of the pipe is considered for the radial shrinkage and measured for four different increments, so that the shrinkage in thickness could be appreciated as shown in Figure 15. At a tilt angle of 45 degrees, the radial shrinkage is 0.022mm, and similarly at at an angle of 27.5 degrees, the radial shrinkage is 0.010mm.

D. Axial Shrinkage

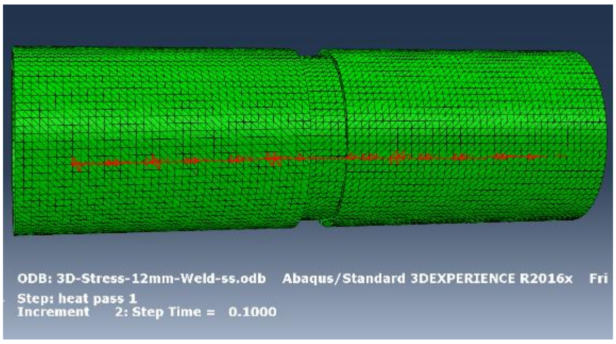

Fig. 17. A typical pipe model showing nodal points for axial shrinkage

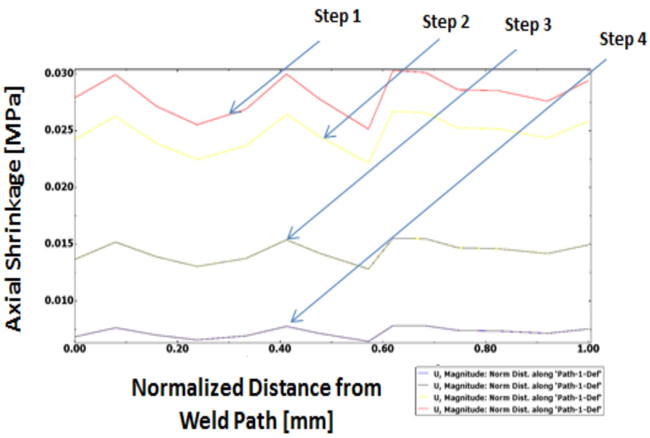

Fig. 18. Axial shrinkage versus normalized distance curve on the outer surface of the HAZ of the 12 mm clad pipes

ISBN: 978-988-14048-3-1
ISSN: 2078-0958 (Print); ISSN: 2078-0966 (Online)

For four different increments of the axial lenght, the shrinkage is measured and plotted against the normalized distance from the weld path. The axial shrinkage at lower increments is slightly different from those at higher increments, because there are high thermal gradients experienced during butt welding leading to residual stress and discrepancy in hardness, hence a creep effect is observed at higher increments.

V. Conclusion

From the various plots of temperature versus distance along the path of weld propagation, it has been observed that the distribution of heat follows a unique pattern which has been displayed in Figures 9 to 11, with the different HAZ being taken into account. The peaks displayed in the plots correspond to the immediate vicinity of the weld, with the number and magnitude of the peaks increasing as the cumulative quantity of heat is dispelled within the weldment, and likewise decreasing the further away one goes form the region of the weld.

From the results of the simulated axial stress and the residual axial stress distributions on the inner surface of the pipe, the following can be deduced:

1. Close to the region of weld region, comprehensive axial, radial and hoop stresses can be observed but farther away from the weld region, tensile stresses become the trend.
2. Also, due to the symmetry across the weld line $W_{L,}$ the axial stresses are symmetric in nature.
3. The radial and axial shrinkage effects on the 12mm cladded pipe also agree with findings from the thermal analysis, tensile stress curve and microstructures of weld.
4. Results from the literature further confirm the validity of the simulations carried out in this research.

Acknowledgment

The authors want to express their gratitude to Brunel University London for the facilities provided and conducive research environment.

The first author also thanks The Petroleum Technology Development Fund (PTDF) for their funding and support through which this research has been made possible.

References

[1] S. Lampman, “Weld Integrity and Performance”, *ASM International*, 2001.
[2] J.A. Goldak, “Computational Welding Mechanics”, *Springer*, 2005.
[3] A.G. Youtsos, “Residual Stress and its Effects on Fatigue and Fracture”, *Springer*, 2006.
[4] E. Muhammad, “Analysis of Residual Stresses and Distortions in Circumferentially Welded Thin-Walled Cylinders*”,* National University of Science and Technology, Pakistan, 2008.
[5] M.E. EDU, “Gaussian Curvature”, retrieved from Math ETSU EDU, December 29, 2016.
[6] C.P. Stone, P. Omnes, R.V.P Rezende, H. Grimm-Strele and R.E Bensow, www.researchgate.net: https://www.researchgate.net/post/Can_somebody_outline_the_advantages_of_utilizing_a_hexahedral_mesh_as_compared_to_a_tetrahedral_mesh2, retrieved September 12, 2016.
[7] D.S. Sun, Q. Liu, M. Brandt, M. Janardhana and G. Clark, “Microstructure and Mechanical Properties of Laser Cladding Repair of AISI 4340 Steel”, *International Congress of the Aeronautical Sciences*, pp. 1-9, 2012.
[8] N.U. Dar, E.M. Qureshi and M.M.I. Hammouda, “Analysis of weld-induced residual stresses and distortions in thin-walled cylinders”, *Journal of Mechanical Science and Technology*, Vol. 23, pp. 1118-1131, 2009.
[9] P.K. Sinha, R. Islam, C. Prasad and M. Kaleem, “Analysis of residual stresses and distortions in girth-welded Carbon steel